Microchimica Acta
https://doi.org/10.1007/s00604-018-2983-3

ORIGINAL PAPER

Impedimetric determination of Staphylococcal enterotoxin B using electrochemical switching with DNA triangular pyramid frustum nanostructure

Xiaoye Chen[1] · Xinping Shi[1] · Yun Liu[1] · Lixia Lu[1] · Yichen Lu[1] · Xiong Xiong[1] · Yuanjian Liu[1] · Xiaohui Xiong[1]

Received: 4 May 2018 / Accepted: 28 August 2018

Abstract

An electrochemical switching strategy is presented for the sensitive determination of *Staphylococcus* enterotoxin B (SEB). It is based on the use of DNA triangular pyramid frustum nanostructure (TPF_{DNA}) consisting of (a) three thiolated probes, (b) one auxiliary probe, and (c) an aptamer against SEB. The TPF_{DNA} was assembled on the gold electrode, with the SEB aptamer designed on top of the TPF_{DNA}. The electron transfer to hexacyanoferrate acting as an electrochemical probe is strongly inhibited in the TPF_{DNA}-modified electrode. This is assumed to be due to the formation of a 3D TPF_{DNA} structure that limits access of hexacyanoferrate to the electrode. Therefore, the Faradaic impedance is large. However, in the presence of SEB, it will bind to the aptamer and dehybridize the hybrid formed between aptamer and its complementary sequence. As a result, the TPF_{DNA} nanostructure changes to an equilateral triangle DNA nanostructure. This results in a more efficient electron transfer and a smaller Faradaic impedance. The method has a detection limit of 0.17 ng mL^{-1} of SEB (at an S/N of 3) and a dynamic range that covers the 0.2–1000 ng mL^{-1} concentration range. The applicability and reliability of the method was demonstrated by anayzing (spiked) milk samples, and the results were compared to those obtained with an ELISA kit. The relative standard deviations between the two methods range between −6.59 and 9.33%.

Keywords Triangular pyramid frustum nanostructure · Aptamer · *Staphylococcus aureus* · Electrochemical biosensor · Gold electrode · Hexacyanoferrate · Electron transfer · Double-layer barrier · Faradaic impedance · ELISA

Introduction

Foodborne illness caused by small thermally stable staphylococcal enterotoxins (SEs) [1], produced by *Staphylococcus aureus* [2], are still one of the most primary issues for human health and food safety [3]. SEs comprised a group of five classical types (SEA, SEB, SEC, SED, SEE) and other new types (SEG-SEV) according to serological types [4]. Among the SEs, staphylococcal enterotoxin B (SEB) with the most thermal stability and strongest toxicity [5] is the most common and can induce gastrointestinal symptoms like diarrhea and emesis [6]. Additionally, SEB was classified into a potential bioweapon agent [7], since it can not only cause breath difficulties and systemic damage, but be aerosolized easily in addition to the high stability. Considering the strong toxic and active effects of SEB with its efficacy (lethal dose 0.02 μg kg^{-1} and emetic response 0.4 ng kg^{-1}) [8]. It would be extremely expected that devising a rapid, sensitive, convenient method for detection of low concentrations SEB.

There are numerous methods and techniques [9–11] for the detection of SEB, such as chromatography [12], colorimetric [13], fluorescent [14], and immunochemical methods [15]. However, high cost, time-consuming, or extensive sample pretreatment procedures limit their practical application. In virtue of these disadvantages of abovementioned methods, immunological methods or biosensors [16] have been emerged as an alternative and attractive tool. The most commonly reported analytical techniques for detection of SEB

Electronic supplementary material The online version of this article (https://doi.org/10.1007/s00604-018-2983-3) contains supplementary material, which is available to authorized users.

✉ Yuanjian Liu
lucias_cumt@163.com

[1] Coll Food Sci & Light Ind, Nanjing Tech University, Nanjing 211816, People's Republic of China

Published online: 15 September 2018

were immunosensors based on antibodies capturing probes. Nevertheless, antibodies are coupled with long preparation period, short term stability upon modification and unstable test result apart from high products cost and depending on environmental conditions for specificity and affinity [17, 18], leading to blocking the extensive applications for on-site detection of SEB. In comparison with antibody, aptamer selected by an in vitro process called as systematic evolution of ligands by exponential enrichment (SELEX) possessed the capacities for high specificity recognition and affinity for a wide range of targets such as toxins and peptides [19]. Therefore, aptamer as single-chain oligonucleotides has been considered as an attractive candidates aiming to replace antibody in a broad range of analytical techniques [20], due to several advantages including its cheap productions, thermal and chemical stability, high sensitivity, simple operation and portable facility. Furthermore, electrochemical aptamers [21] have gained tremendous attention to be used in the fields of food quality control and biomedical diagnosis, owing to rapid response and high sensitivity. In view of the typical properties with specific rigid structure and excellent stability, the double-layer DNA nanostructure emerging as recognition probes assembled on gold surfaces has gained extremely promising attention [22]. Establishment of DNA nanostructure with nearly random 3D nanostructure might brought new, ultrasensitive DNA nanostructure-based biosensors [23] for detection of target analytes relative to traditional linear or stem-loop DNA structures [24].

Sheng et al. have demonstrated an ultrasensitive electrochemical cocaine biosensor based on 3D DNA structure conversion of nanostructure from triangular pyramid frustum (TPF_{DNA}) to equilateral triangle (ET_{DNA}) and a low nanomolar (0.21 nM) detection limit was achieved [25]. With this strategy in mind, we proposed a highly sensitive electrochemical biosensor based on the DNA nanostructure-decorated sensing protocol for the detection of SEB. The transduction protocol utilized the structural change from "Open" and "Close" states to control electron-transfer resistance of $Fe(CN)_6^{3-/4-}$ as indicator across the interface of gold electrode. For practical application, the effectiveness of the biosensor was demonstrated by using spiked skim milk and milk power. Altogether, this sensing protocol provides a rapid, convenient, and highly sensitive and reversible method for the detection of SEB.

Experimental section

Chemicals and materials

The oligonucleotides were purchased from Shanghai Sangon Biological Engineering Technology & Services Co. Ltd. (Shanghai, China, http://www.sangon.com/) and suspended in TE buffer (10 mM Tris, 1 mM EDTA, pH 8.0) to a final concentration of 50 μM. The sequence of synthesized oligonucleotides is given in Table 1.

SEB (catalog number: BT202, highly purified) was gained from Toxin Technology, Inc. (Sarasota, FL, http://www.toxintechnology.com/). ELISA kits of SEB, staphylococcal enterotoxin A (SEA) and staphylococcal enterotoxin C (SEC) were received from Shanghai Jianglai Industrial Limited By Share Ltd. (Shanghai, China, http://www.jonln.com/). Aflatoxin B1 (AFB1) and Ochratoxin A (OTA) were purchased from Academy of State Administration of Grain (Beijing, China, http://www.chinagrain.org/). Chloramphenicol (CAP) was provided from WITEGA Laboratorien Berlin-Adlershof GmbH (Berlin, Germany, http://witega.lookchem.com/). Casein (CS), BSA, and hexaammineruthenium(II) chloride ($[Ru(NH_3)_6]^{3+}$, RuHex) were obtained from Sigma-Aldrich Co. Ltd. (St. Louis, MO, https://www.sigmaaldrich.com/). Tris-(2-carboxyethyl) phosphine hydrochloride (TCEP) was received from Shanghai Macklin Biochemical Co. Ltd. (Shanghai, China, http://macklin.company.lookchem.cn/). Distilled water was used for all of the experiments.

The buffers employed in this study were as follows: Phosphate buffered saline (PBS) solution (8.24 mM Na_2HPO_4, 1.76 mM NaH_2PO_4, 136.89 mM NaCl, 2.67 mM KCl, pH 7.2 ~ 7.4); TM buffer (20 mM Tris, 50 mM $MgCl_2$, pH 8.0); Electrolyte (I) (1 mM $K_3[Fe(CN)_6]/K_4[Fe(CN)_6]$ (1:1) and 100 mM KCl in PBS); Electrolyte (II) (10 mM Tris, 50 μM RuHex, pH 7.4).

Characterization and measurements

A CHI 660D electrochemical workstation was used for all cyclic voltammetry (CV) and chronocoulometry (CC) (Chenhua Instruments, Shanghai, China). A conventional three-electrode system was employed with gold electrode or modified gold electrode as the working electrode, platinum wire as the counter electrode, and Ag/AgCl (3 M KCl) as the reference electrode, respectively. The electrochemical signal was measured with CV by scanning from −0.2 V to 0.8 V (versus Ag/AgCl) in 6 mL of electrolyte (I) solution. Electrochemical impedance spectroscopy (EIS) was performed on a VersaSTAT 3 workstation (Princeton Applied Research, USA). EIS was recorded in electrolyte (I) with a frequency range of 0.01 to 10^5 Hz. CC was performed in electrolyte (II) with the following parameters: initial potential = −0.5 V, final potential = 0.2 V, number of steps = 2, pulse width = 0.5 s, sample interval = 5 ms, quiet time = 2.0 s, sensitivity (C or A/V) = 1e-5 A V^{-1}. EIS was recorded in electrolyte (I) with a frequency range of 0.01 to 10^5 Hz.

Table 1 Sequences of oligonucleotides employed in this work

Name	Sequence and modifications (from 5′-3′)
P1	5'-HS-C6-TTCAGACTTAGGAATGTCATTTTTTTTTTTTACAACAGACAACG-3'
P2	5'-HS-C6-TACTATGGCGGCTCTTCGCTTTTTTTTTTTTCCAGTGGATGCGA-3'
P3	5'-HS-C6-GTGTAGCAAGCTGTAATTCTTTTTTTTTTTTCCTCAATACCAAA-3'
P4	5'-ACATTCCTAAGTCTGAAACATTACAGCTTGCTACACGAGAAGAGCCGCCATAGTA-3'
P5	5'-TTTGGTATTGAGGGTCGCATCCACTGGTCGTTGTCTGTTGTCTGTTATGTTGTTTC GTG ATGGCTCTAACTCTCCTCT-3'

Formation of TPF_{DNA} and fabrication of electrochemical sensor

TPF_{DNA} was formed as reported previously [25]. In brief, equimolar quantities of five oligonucleotides (Table 1) for the formation of the TPF_{DNA} was dissolved in TE buffer, yielding a final concentration of 50 μM. 1 μL of each strand was mixed with 1 μL of TCEP (500 mM) and 44 μL of TM buffer. The resulting mixture was heated to 95 °C for 10 min, then cooled to 4 °C for 30 min using a thermal cycler S1000TM (MJ Research Inc., SA). In this way, SEB aptamer on the top of the TPF_{DNA} and three thiol groups at the other three vertices was constructed.

The cleaned 2 mm diameter gold electrodes (CH Instruments Inc., Shanghai, China) were rinsed with a copious amount of RNase-free water and blown dry with nitrogen. To each pretreated working electrode, 10 μL of various concentrations of TPF_{DNA} in 1 × PBS was added and incubated for 12 h at room temperature for immobilization. Following the incubation, the resulting modified electrodes were rinsed with 1 × PBS and used for the following experiment.

Electrochemical assay of SEB

Various concentrations of SEB was droped on the TPF_{DNA}-modified gold electrodes surfaces and incubation for a certain period of time at room temperature. Then, the electrodes were extensively rinsed and subjected to electrochemical measurements. Additionally, the TPF_{DNA}-modified gold electrodes were exposed to the different concentrations analogs or other common toxins relative to SEB to evaluate the specificity and sensitivity.

Sample treatment

In order to evaluate analytical reliability and application capability of the designed electrochemical biosensor in real samples, skim milk and milk powder were selected as model samples to be tested. All samples were purchased from the local market in Nanjing, China. The steps for sample pretreatment mainly refer to Wu's method [15]: In brief, 25 g milk samples were added to 125 mL Tris buffer, followed by centrifugation at 400 rcf for 10 min. Then, the solution was diluted with 20 mL milk samples/PBS mixture (*v*/v ratio, 1:19). After that, 100 μL of supernatant was collected for the following experiments after removing the fat layer. Finally, to prepare different concentrations of SEB spiked milk samples (1, 5, and 20 ng mL^{-1}), known quantities of ng mL^{-1} SEB standard solution were injected into milk samples in triplicate and a blank spiked experiment with the solvent only was also tested.

Results and discussion

Sensing strategy

The principle of electrochemical switching with DNA triangular pyramid frustum nanostructures for SEB detection is shown in Scheme 1. First, the initial DNA triangular pyramid frustum nanostructure (defined as TPF_{DNA}) was hierarchically

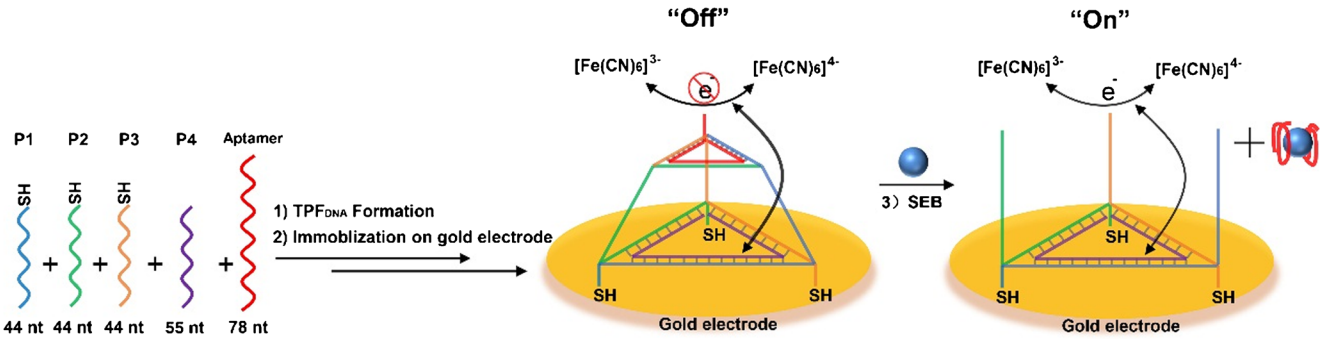

Scheme 1 Schematic illustration of the SEB sensing based on TPF_{DNA} assembled on gold electrode

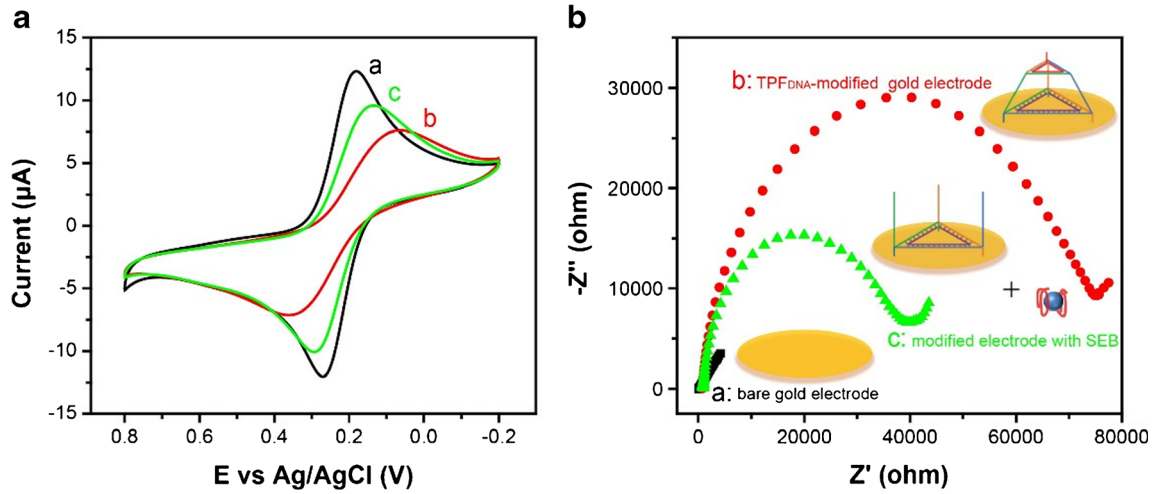

Fig. 1 **a** CV and **b** EIS spectrums of **a** bare gold electrode, **b** TPF_{DNA}-modified gold electrode and **c** modified gold electrode with 10 ng mL^{-1} SEB in 1 × PBS, 1 mM $K_3[Fe(CN)_6]/K_4[Fe(CN)_6]$ (1:1), 100 mM KCl

assembled from three thiolated probes (P1, P2, P3 with 44 bp), one auxiliary probe (P4 with 55 bp) and SEB aptamer (SEB aptamer was designed on the top of the TPF_{DNA}, 78 bp) in TM buffer. In this way, 5′-end of three equal parts of 17-base fragments in P1, P2, and P3 would hybridize with its complementary sequence in P4. Part of SEB aptamer was fully complementary to the 3′-end of the 13-base fragments of P1, P2, and P3 which allowed the formation of a short 13-base DNA duplex at the distal end of the probes. Then TPF_{DNA} assembled onto gold electrode surface by the three thiol groups was formed. In this state, a large Faradaic impedance response of $Fe(CN)_6^{3-/4-}$ was observed, due to the formation of the 3D TPF_{DNA} that prevents $Fe(CN)_6^{3-/4-}$ from accessing the electrode surface for efficient electron transfer. Thus, the TPF_{DNA} can represent a "Close" state of the aptamer-composed DNA nanostructure. Subsequently, in the presence of SEB, the high specific recognition and affinity constants of aptamer and SEB destroyed the hybrid of aptamer and its complementary sequence; as a result, TPF_{DNA} nanostructure changed to an equilateral triangle DNA nanostructure (defined as ET_{DNA}), resulting in an efficient electron transfer and a small Faradaic impedance response of $Fe(CN)_6^{3-/4-}$.

Electrochemical characterization for sensing process of the TPF_{DNA}-modified gold electrode was illustrated by CV and EIS. Fig. 1 shows the CV and EIS for bare gold electrode, TPF_{DNA}-modified gold electrode, and 10 ng mL^{-1} SEB with TPF_{DNA}-modified gold electrode. Without introducing SEB, the DNA triangular pyramid frustum nanostructure on the surface of gold electrode remained intact. Therefore, the redox mediator, $[Fe(CN)_6]^{4-/3-}$, had a limited access to the surface of electrode because of the presence of double-layer barrier on the surface of electrode, so a weak current signal (Fig. 1a,

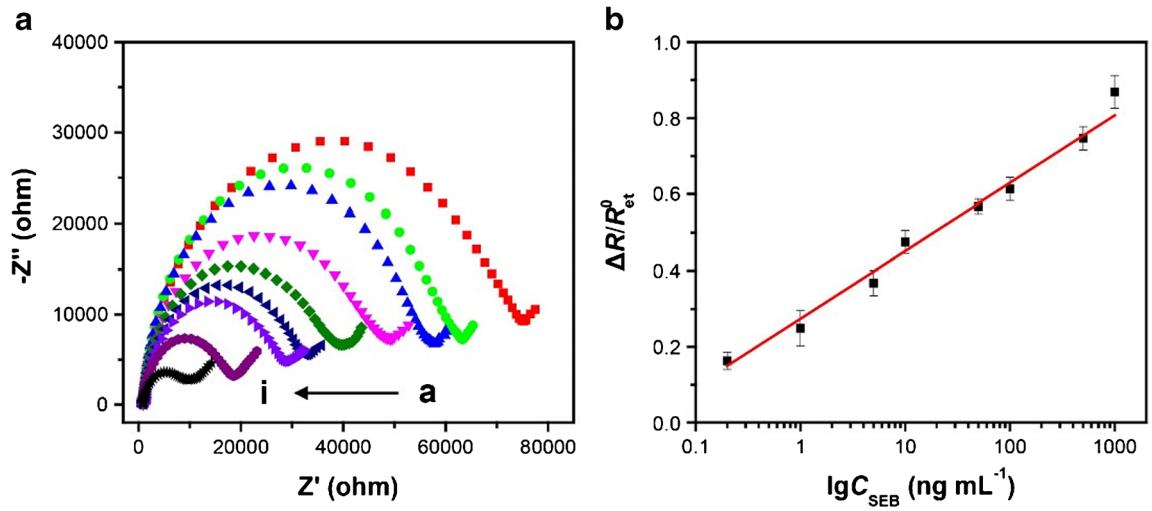

Fig. 2 **a** EIS response curves of the electrochemical biosensor with different concentrations of SEB at (a) 0, (b) 0.2, (c) 1, (d) 5, (e) 10, (f) 50, (g) 100, (h) 500 and (i) 1000 ng mL^{-1} respectively. **b** Variance of ΔR_{et} as a function of the concentration of SEB in the range from 0.2 ng mL^{-1} to 1000 ng mL^{-1}. Error bars showed the standard deviation of three experiments

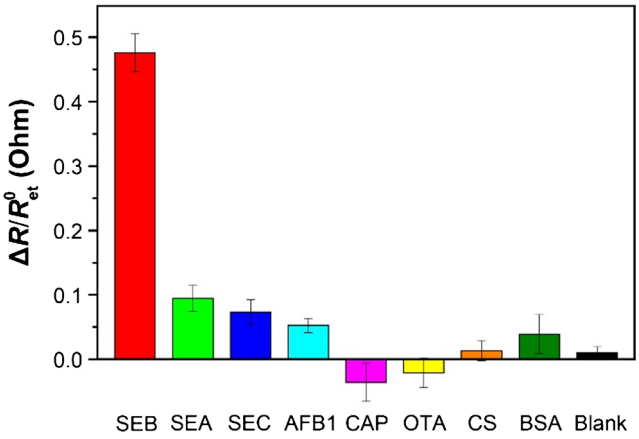

Fig. 3 Selectivity of the sensing system in the presence of SEB, SEA, SEC, AFB1, CAP, OTA, CS and BSA (SEB: 10 ng mL^{-1}, SEA: 20 ng mL^{-1}, SEC: 20 ng mL^{-1}, and 100 ng mL^{-1} for others). Error bars showed the standard deviation of three experiments

curve b) and a large electrontransfer resistance (Fig. 1b, curve b) were measured. In the presence of SEB, aptamer interacted with its target and released from TPF_{DNA}. So, the DNA triangular pyramid frustum nanostructure was disassembled, the current signal was increased (Fig. 1a, curve c) and electrontransfer resistance values was decreased (Fig. 1b, curve b). It has been demonstrated that aptamers bind to their targets with a better binding affinity in contrast to their complementary strands [44, 47–49]. Therefore, these results verified the formation of TPF_{DNA}-modified gold electrode and SEB addition would result in the activation of the DNA nanostructure from "Close" to "Open".

Optimization of method

The following parameters were optimized: (a) Incubation time; (b) Concentration of TPF_{DNA}. Respective data and Fig. S1 are given in the Electronic Supporting Material. The following experimental conditions were found to give best results: (a) Optimal incubation time: 100 min; (b) Optimal concentration: 1.0 μM.

SEB detection using the biosensor

To evaluate the sensitivity of the SEB detection by TPF_{DNA}, various concentrations of SEB were examined under optimized conditions. Fig. 2a displays the EIS signal intensity decreased monotonically with the logarithm of the SEB concentration. SEB addition would result in the activation of the DNA nanostructures from "Close" to "Open". Furthermore, As shown in Fig. 2b, the calibration plot obtained by plotting the $\Delta R/R^0_{et}$ versus the logarithm of the SEB concentration, showed a good linearity relationship in the range from 0.2 ng mL^{-1} to 1000 ng mL^{-1} ($R^2 = 0.9944$) with the detection limit of 0.17 ng mL^{-1} ($S/N = 3$). Moreover, to get a clear perspective of the performance of the proposed method, a comparison between the proposed method and some of the previously reported methods was shown in Table S1. The detection limit of this method was better or comparable to most previously reported methods, and it also exhibited higher sensitivity, a wider linear range for SEB detection.

Selectivity of the sensing system

Selectivity, a fundamental factor, is usually considered for new detection strategy. To explore the selectivity of the sensing method, some analogs (SEA, SEC) and other common toxins (AFB1, CAP, OTA, CS, BSA) were chosen for specificity comparison. Fig. 3 shows that only SEB gives a remarkable impedimetric response, while the potential interferents give a negligible signal. This result verified that the established electrochemical switching strategy had extraordinary selectivity toward SEB.

Assay of SEB in skim milk and milk powder

A significant and challenging factor for SEB analysis is the applicability in complex food matrices. The skim milk and milk power samples spiked with 1, 5 and 20 ng mL^{-1} SEB, respectively, were analyzed using the method and the ELISA kit. The results are shown in Table 2. The relative deviation

Table 2 Recoveries of SEB in food samples for applicability of biosensor and the ELISA kit

Sample	Original (ng mL^{-1})	Added (ng mL^{-1})	Found (ng mL^{-1})		Relative deviation[b] (%)
			ELISA (mean ± SD)	Biosensor[a] (mean ± SD)	
Skim milk	0	1	0.85 ± 0.07	0.91 ± 0.04	−6.59
		5	5.27 ± 0.12	4.82 ± 0.14	9.33
		20	20.38 ± 0.32	19.61 ± 0.41	3.93
Milk powder	0	1	1.03 ± 0.19	0.95 ± 0.08	8.42
		5	4.82 ± 0.21	5.11 ± 0.25	−5.68
		20	20.22 ± 0.33	19.25 ± 0.32	5.04

a: Each data point present an average of five independent measurements

b: Relative deviation $(\%) = \frac{\text{Found}_{\text{ELISA}} - \text{Found}_{\text{Biosensor}}}{\text{Found}_{\text{Biosensor}}} \times 100\%$

between the two methods ranged from −6.59 to 9.33%, which indicates that there is no significant difference between the results given by the two methods. However, other biomolecules or food matrix effects have limited this electrochemical method's performance on raw biological sample.

Conclusion

In summary, a novel electrochemical switching strategy based on the structure conversion of TPF_{DNA} was designed for detection of SEB in this study. Owing to the uniquely structural features, the prepared biosensor exhibited high sensitivity, selectivity, reproducibility and low detection limits. Additionally, the sensing method may be applied to detect SEB in real samples (the skim milk and milk power). The relative deviation between this assay and the ELISA kit was in the range of −6.59% ~ 9.33%, indicating that this electrochemical method can reveal the promising applications for the on-site analysis of SEB. This electrochemical method is suffering from to be affected by other biomolecules or food matrix effects.

Acknowledgements The project was supported by the National Natural Science Foundation of China (grant no. 31701688, 21707070), and the Natural Science Foundation of Jiangsu Province of China (grant no. BK20170998).

Compliance with ethical standards The author(s) declare that they have no competing interests.

References

1. Pinchuk IV, Beswick EJ, Reyes VE (2010) Staphylococcal enterotoxins. Toxins 2:2177–2197. https://doi.org/10.3390/toxins2082177
2. Wang HW, Wang HH, Liang LJ, Xu XL, Zhou GH (2018) Prevalence, genetic characterization and biofilm formation in vitro of Staphylococcus aureus isolated from raw chicken meat at retail level in Nanjing, China. Food Control 86:11–18. https://doi.org/10.1016/j.foodcont.2017.10.028
3. Nunes MM, Caldas ED (2017) Preliminary quantitative microbial risk assessment for Staphylococcus enterotoxins in fresh minas cheese, a popular food in Brazil. Food Control 73:524–531. https://doi.org/10.1016/j.foodcont.2016.08.046
4. Fisher EL, Otto M, Cheung GYC (2018) Basis of virulence in enterotoxin-mediated staphylococcal food poisoning. Front Microbiol 9(436). https://doi.org/10.3389/fmicb.2018.00436
5. Wang WB, Wang WW, Liu LQ, Xu LG, Kuang H, Zhu JP, Xu CL (2016) Nanoshell-enhanced Raman spectroscopy on a microplate for staphylococcal enterotoxin B sensing. ACS Appl Mater Interfaces 8:15591–15597. https://doi.org/10.1021/acsami.6b02905
6. Sorensen M, Klingenberg C, Wickman M, Sollid JUE, Furberg AS, Bachert C, Bousquet J (2017) Staphylococcus aureus enterotoxin sensitization is associated with allergic poly-sensitization and allergic multimorbidity in adolescents. Allergy 72:1548–1555. https://doi.org/10.1111/all.13175
7. Singh PK, Agrawal R, Kamboj DV, Gupta G, Boopathi M, Goel AK, Singh L (2010) Construction of a single-chain variable-fragment antibody against the superantigen staphylococcal enterotoxin B. Appl Environ Microbiol 76:8184–8191. https://doi.org/10.1128/AEM.01441-10
8. Deng RN, Wang L, Yi GZ, Hua EH, Xie GM (2014) Target-induced aptamer release strategy based on electrochemical detection of staphylococcal enterotoxin B using GNPs-ZrO_2-chits film. Colloid Surf B 120:1–7. https://doi.org/10.1016/j.colsurfb.2014.04.028
9. Wu SJ, Duan N, Gu HJ, Hao LL, Ye H, Gong WH, Wang ZP (2016) A review of the methods for detection of Staphylococcus aureus enterotoxins. Toxins 8:176. https://doi.org/10.3390/toxins8070176
10. Rodriguez A, Gordillo R, Andrade MJ, Cordoba JJ, Rodriguez M (2016) Development of an efficient real-time PCR assay to quantify enterotoxin-producing staphylococci in meat products. Food Control 60:302–308. https://doi.org/10.1016/j.foodcont.2015.07.040
11. Ludwig S, Jimenez-Bush I, Brigham E, Bose S, Diette G, McCormack MC, Matsui EC, Davis MF (2017) Analysis of home dust for Staphylococcus aureus and staphylococcal enterotoxin genes using quantitative PCR. Sci Total Environ 581:750–755. https://doi.org/10.1016/j.scitotenv.2017.01.003
12. Andjelkovic M, Tsilia V, Rajkovic A, De Cremer K, VanLoco J (2016) Application of LC-MS/MS MRM to determine staphylococcal enterotoxins (SEB and SEA) in milk. Toxins 8:118. https://doi.org/10.3390/toxins8040118
13. Mondal B, Bhavanashri N, Ramial S, Kingston J (2018) Colorimetric DNAzyme biosensor for convenience detection of enterotoxin B harboring Staphylococcus aureus from food samples. J Agric Food Chem 66:1516–1522. https://doi.org/10.1021/acs.jfc.7b04820
14. Wang XL, Huang YK, Wu SJ, Duan N, Xu BC, Wang ZP (2016) Simultaneous detection of Staphylococcus aureus and Salmonella typhimurium using multicolor time-resolved fluorescence nanoparticles as labels. Int J Food Microbiol 237:172–179. https://doi.org/10.1016/j.ijfoodmicro.2016.08.028
15. Wu LY, Gao B, Zhang F, Sun XL, Zhang YZ, Li ZJ (2013) A novel electrochemical immunosensor based on magnetosomes for detection of staphylococcal enterotoxin B in milk. Talanta 106:360–366. https://doi.org/10.1016/j.talanta.2012.12.053
16. Seshadri P, Manoli K, Schneiderhan-Marra N, Anthes U, Wierzchowiec P, Bonrad K, DiFranco CD, Torsi L (2018) Low-picomolar, label-free procalcitonin analytical detection with an electrolyte-gated organic field-effect transistor based electronic immunosensor. Biosens Bioelectron 104:113–119. https://doi.org/10.1016/j.bios.2017.12.041
17. Abnous K, Danesh NM, Alibolandi M, Ramezani M, Emrani AS, Zolfaghari R, Taghdisi SM (2017) A new amplified π-shape electrochemical aptasensor for ultrasensitive detection of aflatoxin B1. Biosens Bioelectron 94:374–379. https://doi.org/10.1016/j.bios.2017.03.028
18. Zheng WL, Teng J, Cheng L, Ye YW, Pan DD, Wu JJ, Xue F, Liu GD, Chen W (2016) Hetero-enzyme-based two-round signal amplification strategy for trace detection of aflatoxin B1 using an electrochemical aptasensor. Biosens Bioelectron 80:574–581. https://doi.org/10.1016/j.bios.2016.01.091
19. Nguyen VT, Kwon YS, Gu MB (2017) Aptamer-based environmental biosensors for small molecule contaminants. Curr Opin Biotechnol 45:15–23. https://doi.org/10.1016/j.copbio.2016.11.020
20. Mondal B, Ramlal S, Lavu PS, Bhavanashri N, Kingston J (2018) Highly sensitive colorimetric biosensor for staphylococcal enterotoxin B by a label-free aptamer and gold nanoparticles. Front Microbiol 9(179). https://doi.org/10.3389/fmicb.2018.00179
21. Hasanzadeh M, Shadjou N, delaGuardia M (2017) Aptamer-based assay of biomolecules: recent advances in electro-analytical approach. Trac-Trend Anal Chem 89:119–132. https://doi.org/10.1016/j.trac.2017.02.003

22. Zeng Y, Zhang D, Qi P, Zheng LB (2017) Colorimetric detection of DNA by using target catalyzed DNA nanostructure assembly and unmodified gold nanoparticles. Microchim Acta 184:4809–4815. https://doi.org/10.1007/s00604-017-2463-1
23. Huang RR, He NY, Li ZY (2018) Recent progresses in DNA nanostructure-based biosensors for detection of tumor markers. Biosens Bioelectron 109:27–34. https://doi.org/10.1016/j.bios.2018.02.053
24. Taghdisi SM, Danesh NM, Ramezani M, Emrani AS, Abnous K (2016) A novel electrochemical aptasensor based on Y-shape structure of dual-aptamer-complementary strand conjugate for ultrasensitive detection of myoglobin. Biosens Bioelectron 80:532–537. https://doi.org/10.1016/j.bios.2016.02.029
25. Sheng QL, Liu RX, Zhang S, Zheng JB (2014) Ultrasensitive electrochemical cocaine biosensor based on reversible DNA nanostructure. Biosens Bioelectron 51:191–194. https://doi.org/10.1016/j.bios.2013.07.053